ANL/ET/CP - 95218

Effects of LWR Coolant Environments on Fatigue Lives of Austenitic Stainless Steels*

Omesh K. Chopra and Daniel J. Gavenda
Energy Technology Division
Argonne National Laboratory
9700 South Cass Avenue
Argonne, Illinois 60439 USA

November 1997

Submitted for publication in the Journal of Pressure Vessel Technology.

---

*Work supported by the Office of Nuclear Regulatory Research of the U.S. Nuclear Regulatory Commission, under FIN Number W6610; Program Manager: Dr. M. McNeil.

Effects of LWR Coolant Environments on Fatigue Lives of Austenitic Stainless Steels

Omesh K. Chopra and Daniel J. Gavenda
Energy Technology Division
Argonne National Laboratory
Argonne, Illinois 60439

Abstract

Fatigue tests have been conducted on Types 304 and 316NG stainless steels to evaluate the effects of various material and loading variables, e.g., steel type, strain rate, dissolved oxygen (DO) in water, and strain range, on the fatigue lives of these steels. The results confirm significant decreases in fatigue life in water. Unlike the situation with ferritic steels, environmental effects on Types 304 and 316NG stainless steel are more pronounced in low-DO than in high-DO water. Experimental results have been compared with estimates of fatigue life based on a statistical model. The formation and growth of fatigue cracks in air and water environments are discussed.

Introduction

The ASME Boiler and Pressure Vessel Code Section III, Subsection NB, which contains rules for the construction of Class 1 components for nuclear power plants, recognizes fatigue as a possible mode of failure in pressure vessel steels and piping materials. Cyclic loadings on a structural component occur because of changes in mechanical and thermal loadings as the system goes from one load set (e.g., pressure, temperature, moment, and force loading) to any other load set. For each pair of load sets, an individual fatigue usage factor is determined by the ratio of the number of cycles anticipated during the lifetime of the component to the allowable cycles. Figures I-9.1 through I-9.6 of Appendix I to Section III of the Code specify fatigue design curves that define the allowable number of cycles as a function of applied stress amplitude. The cumulative usage factor (CUF) is the sum of the individual usage factors. The ASME Code Section III requires that the CUF at each location must not exceed 1.

Subsection NB-3121 of Section III of the Code states that the data on which the fatigue design curves are based did not include tests in the presence of corrosive environments that might accelerate fatigue failure. Article B-2131 in Appendix B to Section III states that the owner's design specifications should provide information about any reductions to fatigue design curves that are necessitated by environmental conditions. Recent fatigue strain-vs.-life (S-N) data illustrate potentially significant effects of light water reactor (LWR) coolant environments on the fatigue resistance of pressure vessel and piping materials (Chopra and Shack, 1995, 1997; Higuchi and Iida, 1991; Higuchi et al., 1995; Mimaki et al., 1996; Shack and Burke, 1991). Therefore, the margins in the ASME Code may be less conservative than originally intended.

A program is being conducted at Argonne National Laboratory (ANL) to provide data and models for predicting environmental effects on fatigue design curves and to assess the validity of fatigue damage summation in piping and vessel steels under load histories typical of LWR components. Based on the existing fatigue S-N data, interim fatigue design curves that address environmental effects on fatigue life of carbon and low-alloy steels and austenitic stainless steels (SSs) have been proposed by Majumdar et al. (1993). Statistical models have

been developed by Keisler et al., (1995, 1996) for estimating the effects of various material and loading conditions on fatigue lives of materials used in the construction of nuclear power plant components.

This paper presents fatigue data on austenitic SSs under conditions that are not addressed by the existing S–N data base. Fatigue tests have been conducted on Types 304 and 316NG SS in air and LWR environments to evaluate the effects of material and loading variables such as steel type, strain rate, dissolved oxygen (DO) in water, and strain range, on the fatigue lives of these steels. Experimental results have been compared with estimates of fatigue life based on a statistical model. The formation and growth of fatigue cracks in austenitic SSs in air and LWR environments are discussed.

Experimental

Fatigue tests have been conducted on Types 316NG and 304 SS to establish the effects of LWR coolant environments on fatigue lives of these steels. The composition of the two steels is given in Table 1. Smooth cylindrical specimens with 9.5–mm diameter and 19–mm gauge length were used for the fatigue tests. All tests were conducted at 288°C with fully reversed axial loading (i.e., R = –1) and a triangular or sawtooth waveform. Details about the test facility and procedure have been described by Chopra et al. (1995). Tests in water were conducted in a small autoclave under stroke control where the specimen strain was controlled between two locations outside the autoclave. Tests in air were performed under strain control with an axial extensometer; specimen strain between the two locations used in the water tests was also recorded. Information from the air tests was used to determine the stroke that was required to maintain constant strain in the specimen gauge length for tests in water; the stroke is gradually increased during the test to account for cyclic hardening of the material and to maintain constant strain in the specimen gauge section.

Air Environment

Existing fatigue S–N data indicate that the fatigue lives of austenitic SSs in air are independent of temperature in the range from room temperature to 427°C. Fatigue lives of Types 304 and 316 SS are similar and those of Type 316NG are superior. The effects of strain rate on fatigue life cannot be established from the existing S–N data. Limited results suggest that some heats are sensitive to strain rate; fatigue life may decrease up to 30% with decreasing strain rate.

Statistical models have been developed for estimating the effects of material and loading conditions on the fatigue lives of austenitic SSs (Keisler et al., 1995, 1996). These models are based on the JNUFAD* data base for "Fatigue Strength of Nuclear Plant Component" from Japan, the data compiled by Jaske and O'Donnell (1977) for developing fatigue design criteria for pressure vessel alloys, and the tests conducted by Conway et al. (1975), Keller (1977), and Shack and Burke (1991). In air, the fatigue life N of Types 304 and 316 SS is expressed in terms of the strain amplitude ε_a (%) by

$$\ln(N) = 6.690 - 1.980 \ln(\varepsilon_a - 0.12) \qquad (1a)$$

* Private communication from M. Higuchi, Ishikawajima–Harima Heavy Industries Co., Japan, to M. Prager of the Pressure Vessel Research Council, 1992.

that of Type 316NG SS, by

$$\ln(N) = 7.072 - 1.980 \ln(\varepsilon_a - 0.12). \quad (1b)$$

The fatigue lives of Types 304, 316, and 316NG SSs in air at various temperatures and values estimated from Eqs. 1a and 1b are presented in Fig. 1. At temperatures of 25–450°C, the fatigue lives of Types 304 and 316 SS in air show no dependence on temperature. The ANL statistical model shows good agreement with the Jaske and O'Donnell (1977) average curve. Also, note that the ASME mean curve is not consistent with the existing fatigue S–N data for austenitic SSs. At strain amplitudes <0.5%, the mean curve predicts significantly longer fatigue lives than those observed experimentally. When the ASME fatigue S–N curve for austenitic SSs was extended to 10^8 cycles, account was taken of this discrepancy, but no change was made to the curve for $<10^6$ cycles.

The cyclic strain hardening of Type 316NG tested in air at room temperature and 288°C is shown in Fig. 2. At both temperatures, the steel exhibits rapid hardening during the first 50–100 cycles of fatigue life. The extent of hardening increases with applied strain range and is greater at room temperature than at 288°C. The initial hardening is followed by softening and a saturation stage at 288°C and by continuous softening at room temperature. Also, cyclic stresses increase with decreasing strain rate. Type 304 SS shows identical cyclic hardening.

The existing cyclic–stress–vs.–strain data for the various steels indicate that cyclic stresses increase in the following order; Types 316NG, 304, and 316. Furthermore, cyclic stresses are 20–30% lower at 288–430°C than at room temperature. At room temperature, the strain amplitude ε_a(%) can be expressed in terms of the cyclic stress amplitude σ_a(MPa) for Type 316 SS by

$$\varepsilon_a = \frac{\sigma_a}{1950} + \left(\frac{\sigma_a}{588.5}\right)^{1.94}, \quad (2a)$$

for Type 304 SS by

$$\varepsilon_a = \frac{\sigma_a}{1950} + \left(\frac{\sigma_a}{503.2}\right)^{2.19}, \quad (2b)$$

and for Type 316NG by

$$\varepsilon_a = \frac{\sigma_a}{1950} + \left(\frac{\sigma_a}{447.0}\right)^{2.59}. \quad (2c)$$

At 288–430°C, the cyclic stress vs. strain curve can be expressed for Type 316 SS by

$$\varepsilon_a = \frac{\sigma_a}{1760} + \left(\frac{\sigma_a}{496.8}\right)^{2.19}, \quad (2d)$$

for Type 304 SS by

$$\varepsilon_a = \frac{\sigma_a}{1760} + \left(\frac{\sigma_a}{373.9}\right)^{2.31}, \quad (2e)$$

and for Type 316NG by

$$\varepsilon_a = \frac{\sigma_a}{1760} + \left(\frac{\sigma_a}{330.1}\right)^{3.24}. \quad (2f)$$

Water Environment

Fatigue Life. The fatigue S–N data on austenitic SSs indicate a significant decrease in fatigue life in water. The effect of environment on fatigue life increases as strain rate decreases. Statistical models based on the available fatigue S–N data have also been developed at ANL for estimating the fatigue lives of austenitic SSs in LWR environments (Keisler et al., 1995, 1996). The primary sources of relevant S–N data for austenitic SSs are the JNUFAD data base, and the tests conducted by Hale et al. (1977, 1981) in a test loop at the Dresden 1 reactor and by Shack and Burke (1991) at ANL. However, most of the data used to develop the statistical models were obtained in water that contained DO levels that were 0.2 ppm or higher and at temperatures in the range of 288–320°C. Consequently, the models do not consider the effects of temperature or DO content on the fatigue lives of these steels. In LWR environments, the fatigue life N of Types 304 and 316 SS is expressed as

$$\ln(N) = 6.331 - 1.980 \ln(\varepsilon_a - 0.12) + 0.134\ \dot{\varepsilon}^* \qquad (3a)$$

and that of Type 316NG as

$$\ln(N) = 6.713 - 1.980 \ln(\varepsilon_a - 0.12) + 0.134\ \dot{\varepsilon}^*, \qquad (3b)$$

where ε_a is applied strain amplitude (%) and $\dot{\varepsilon}^*$ is transformed strain rate defined as

$$\begin{aligned} \dot{\varepsilon}^* &= 0 && (\dot{\varepsilon} > 1\ \%/s) \\ \dot{\varepsilon}^* &= \ln(\dot{\varepsilon}) && (0.001 \le \dot{\varepsilon} \le 1\ \%/s) \\ \dot{\varepsilon}^* &= \ln(0.001) && (\dot{\varepsilon} < 0.001\ \%/s). \end{aligned} \qquad (3c)$$

The ANL statistical model is recommended for predicting fatigue lives that are $\le 10^6$ cycles. The lower-bound value of 0.001%/s on the strain rate effect was based on the results for carbon and low-alloy steels (Chopra and Shack, 1995, 1997).

The fatigue S–N data for Types 316NG and 304 SS in water at 288°C are shown in Fig. 3; the ASME Code fatigue design curve is also shown in the figure. The results indicate a significant decrease in fatigue life in water when compared with that in air; the reduction in life depends both on strain rate and on the DO content of the water. The fatigue lives of Types 316NG and 304 SS in air, simulated pressurized water reactor (PWR) environment, and high–DO water are plotted as a function of strain rate in Fig. 4. In all of the environments, the fatigue lives of these steels decrease with decreasing strain rate. The effect of strain rate is the smallest in air and largest in a low-DO PWR environment. In a simulated PWR environment, a decrease in strain rate from 0.4 to 0.004%/s decreases fatigue life by a factor of ≈8. The decrease in life is lower at low strain ranges, e.g., a factor of ≈8 at 0.75% and ≈5 at 0.3% strain range.

The results also indicate that environmental effects on the fatigue lives of austenitic SSs are more pronounced in low-DO than in high-DO water. At slow strain rates, e.g., ≈0.004%/s, the reduction in fatigue life is greater by a factor of ≈2 in a simulated PWR environment (<10 ppb DO) than in high-DO water (≥200 ppb DO). Such a dependence of fatigue life on DO content is quite different from that of ferritic steels. For carbon and low-alloy steels, environmental effects on fatigue life increase with increasing DO content above a minimum

threshold value of 0.05 ppm. Also, environmental effects on the fatigue life of carbon and low-alloy steels are modest at DO levels below 0.05 ppm, i.e., fatigue life is lower by a factor of <2 at these levels than it is in air. In view of these results, the statistical models for austenitic SSs (Eqs. 3a–3c) will be updated to incorporate the effects of DO and strain rate on fatigue life.

Metallographic Examination. A detailed examination of the fatigue test specimens was conducted to investigate the role of high-temperature oxygenated water in fatigue cracking. In general, the specimens tested in air show slight discoloration, whereas the specimens tested in oxygenated water developed a gray/black corrosion scale. X-ray diffraction analyses of specimens tested in water indicate that the corrosion scale primarily consists of magnetite (Fe_3O_4) or ferroferric oxide ($FeFe_2O_4$), chromium oxide (CrO), and maghemite (γ-Fe_2O_3). In addition to these phases, a specimen tested in high-DO water also contained hematite (ferric oxide or α-Fe_2O_3).

Figure 5 shows photomicrographs of the fracture surface at approximately the same positions along the crack length for Type 316NG specimens tested in air, high-DO water, and low-DO PWR water. Fatigue striations can be seen clearly on all specimens. The spacing between striations indicates that crack growth rates increase in the following sequence: air, high-DO water, and low-DO PWR water.

The formation and growth of surface cracks in simulated PWR water appear to differ from surface crack formation and growth in air. In all environments, cracks primarily form within persistent slip bands (PSBs). During cyclic straining, strain localization in PSBs results in the formation of extrusions and intrusions at the surface; ultimately, with continued cycling, microcracks develop in these PSBs. Once a microcrack is formed, it continues to grow along its slip plane as a Mode II (shear) crack in Stage I growth. The orientation of the crack is usually at an angle of 45° to the stress axis. The Stage I crack may extend across several grains before the increasing stress intensity of the crack promotes slip on systems other than the primary slip. Because slip is then no longer confined to planes at 45° to the stress axis, the crack begins to propagate as a Mode I (tensile) crack, normal to the stress axis, in Stage II growth. This behavior was observed in all of the specimens tested in air and in most instances for specimens tested in high-DO water. However, in a simulated PWR environment (<10 ppb DO), the surface cracks appear to grow entirely as Mode I tensile cracks normal to the stress axis, Fig. 6.

The enhanced crack growth rates of pressure vessel and piping materials in LWR environments have been attributed to either slip dissolution/oxidation (Ford et al., 1993) or hydrogen-induced cracking (Hänninen et al., 1986) mechanisms. The requirements of slip dissolution/oxidation are that a protective oxide film is thermodynamically stable to ensure that a crack will propagate with a high aspect ratio without degrading into a blunt pit, and that a strain increment occurs to rupture the film, thereby exposing the underlying matrix to the environment. Once the passive oxide film is ruptured, crack extension is controlled by dissolution of freshly exposed surfaces and the oxidation characteristics. Hydrogen-induced cracking of low-alloy steels occurs when hydrogen produced by the oxidation reaction at or near the crack tip is partly absorbed into the metal; the absorbed hydrogen diffuses ahead of the crack tip and interacts with MnS inclusions, leading to formation of cleavage cracks at the inclusion matrix interface; and linkage of the cleavage cracks results in discontinuous crack extension in addition to that caused by mechanical fatigue. Both mechanisms depend on oxide rupture, passivation rates, and liquid diffusion rates. Therefore, it is difficult to differentiate between the two mechanisms. The presence of well-defined fatigue striations suggests that hydrogen-induced cracking may be responsible for environmentally assisted reduction in

fatigue lives of austenitic SSs. Fatigue tests are in progress to characterize the formation and growth of surface cracks in LWR environments.

Conclusions

The existing fatigue S–N data for austenitic stainless steels indicate that the fatigue lives of Types 304 and 316 SS are comparable and those of Type 316NG are superior. In air, the fatigue lives of austenitic SSs are independent of temperature in the range from room temperature to 427°C. Limited results suggest that some heats are sensitive to strain rate. For the various steels, cyclic stresses increase with decreasing strain rate and are 20–30% lower at 288–430°C than at room temperature. The results indicate that the current ASME mean curve is not consistent with existing fatigue S–N data for austenitic SSs.

Fatigue tests have been conducted on Types 316NG and 304 SS to establish the effects of LWR coolant environments on fatigue lives of these steels. The results indicate a significant decrease in fatigue life in water relative to that in air; the decrease in life depends both on strain rate and DO content of the water. Environmental effects on fatigue life are the same for Types 304 and 316NG austenitic SS. However, unlike carbon and low–alloy steels, environmental effects are more pronounced in low–DO than in high–DO water. At a strain rate of ≈0.004%/s, reduction in fatigue life in water that contains <10 ppb DO is greater by a factor of ≈2 than in water that contains ≥200 ppb DO.

Metallographic examination of the fatigue test specimens indicates that hydrogen–induced cracking may be responsible for the reduction in fatigue life of austenitic SSs in LWR environments. The fracture surfaces show well–defined fatigue striations; the striation spacing increases in the following sequence: air, high–DO water, and low–DO PWR water. In air and for most cases in high–DO water, surface cracks initially grow along their slip plane as shear cracks in Stage I growth along planes at 45° to the stress axis; however, in low–DO water, the surface cracks appear to grow entirely as tensile cracks in Stage II growth normal to the stress axis.

Acknowledgments

The authors are grateful to W. F. Burke, T. M. Galvin, and J. Tezack for their contributions to the experimental effort. This work was sponsored by the Office of Nuclear Regulatory Research, U.S. Nuclear Regulatory Commission, FIN Number W6610; Program Manager: Dr. M. McNeil.

References

Chopra, O. K., and Shack, W. J., 1995, "Effects of LWR Environments on Fatigue Life of Carbon and Low–Alloy Steels," *Fatigue and Crack Growth: Environmental Effects, Modeling Studies, and Design Considerations*, PVP Vol. 306, S. Yukawa, ed., American Society of Mechanical Engineers, New York, pp. 95–109.

Chopra, O. K., and Shack, W. J., 1997, "Evaluation of Effects of LWR Coolant Environments on Fatigue Life of Carbon and Low–Alloy Steels," *Proceedings of Symposium on Effects of the Environment on the Initiation of Crack Growth*, ASTM STP 1298, American Society for Testing and Materials, Philadelphia, pp. 247–266.

Conway, J. B., Stentz, R. H., and Berling, J. T., 1975, *Fatigue, Tensile, and Relaxation Behavior of Stainless Steels*, TID–26135, U.S. Atomic Energy Commission, Washington, DC.

Ford, F. P., Ranganath, S., and Weinstein, D., 1993, *Environmentally Assisted Fatigue Crack Initiation in Low-Alloy Steels - A Review of the Literature and the ASME Code Design Requirements*, EPRI Report TR-102765.

Hale, D. A., Wilson, S. A., Kiss, E., and Gianuzzi, 1977, A. J., *Low Cycle Fatigue Evaluation of Primary Piping Materials in a BWR Environment*, GEAP-20244, U.S. Nuclear Regulatory Commission.

Hale, D. A., Wilson, S. A., Kass, J. N., and Kiss, E., 1981, "Low Cycle Fatigue Behavior of Commercial Piping Materials in a BWR Environment," *Journal of Engineering Material Technology*, Vol. 103, pp. 15-25.

Hänninen, H., Törrönen, K., and Cullen, W. H., 1986, "Comparison of Proposed Cyclic Crack Growth Mechanisms of Low Alloy Steels in LWR Environments," *Proceedings 2nd Int. Atomic Energy Agency Specialists' Meeting on Subcritical Crack Growth*, NUREG/CP-0067, MEA-2090, Vol. 2, pp. 73-97.

Higuchi, M., and Iida, K., 1991, "Fatigue Strength Correction Factors for Carbon and Low-Alloy Steels in Oxygen-Containing High-Temperature Water," *Nuclear Engineering Design*, Vol. 129, pp. 293-306.

Higuchi, M., Iida, K., and Asada, Y., 1995, "Effects of Strain Rate Change on Fatigue Life of Carbon Steel in High-Temperature Water," *Fatigue and Crack Growth: Environmental Effects, Modeling Studies, and Design Considerations*, PVP Vol. 306, S. Yukawa, ed., American Society of Mechanical Engineers, New York, pp. 111-116.

Jaske, C. E., and O'Donnell, W. J., 1977, "Fatigue Design Criteria for Pressure Vessel Alloys," *ASME Journal of Pressure Vessel Technology*, Vol. 99, pp. 584-592.

Keisler, J., Chopra, O. K., and Shack, W. J., 1995, *Fatigue Strain-Life Behavior of Carbon and Low-Alloy Steels, Austenitic Stainless Steels, and Alloy 600 in LWR Environments*, NUREG/CR-6335, ANL-95/15.

Keisler, J. M., Chopra, O. K., and Shack, W. J., 1996, "Fatigue Strain-Life Behavior of Carbon and Low-Alloy Steels, Austenitic Stainless Steels, and Alloy 600 in LWR Environments," *Nuclear Engineering Design*, Vol. 167, pp. 129-154.

Keller, D. L., 1977, *Progress on LMFBR Cladding, Structural, and Component Materials Studies During July, 1971 through June, 1972, Final Report, Task 32*, Battelle-Columbus Laboratories, BMI-1928.

Majumdar, S., Chopra, O. K., and Shack, W. J., 1993, *Interim Fatigue Design Curves for Carbon, Low-Alloy, and Austenitic Stainless Steels in LWR Environments*, NUREG/CR-5999, ANL-93/3.

Mimaki, H., Kanasaki, H., Suzuki, I., Koyama, M., Akiyama, M., Okubo, T., and Mishima, Y., 1996, "Material Aging Research Program for PWR Plants," *Aging Management Through Maintenance Management*, PVP Vol. 332, I. T. Kisisel, ed., American Society of Mechanical Engineers, New York, pp. 97-105.

Shack, W. J., and Burke, W. F., 1991, "Fatigue of Type 316NG SS," *Environmentally Assisted Cracking in Light Water Reactors, Semiannual Report, October 1989-March 1990*, NUREG/CR-4667 Vol. 10, ANL-91/5, pp. 3-19.

Table 1. Composition (wt.%) of austenitic stainless steels used for fatigue tests

Material	Heat	Source	C	P	S	Si	Cr	Ni	Mn	Mo	Cu	N
Type 316NG[a]	D432804	Vendor	0.011	0.020	0.001	0.52	17.55	13.00	1.76	2.49	0.10	0.108
		ANL	0.013	0.020	0.002	0.49	17.54	13.69	1.69	2.45	0.10	0.105
Type 304[b]	30956	Vendor	0.060	0.019	0.007	0.48	18.99	8.00	1.54	0.44	–	0.100

[a]ASME SA312 seamless stainless steel pipe (hot finished), 610 mm O.D. and 30.9 mm wall, fabricated by Sumitomo Metal Industries, Ltd. Solution-annealed at 1038–1093°C for 0.5 h and water-quenched.
[b]Solution-annealed at 1050°C for 0.5 h.

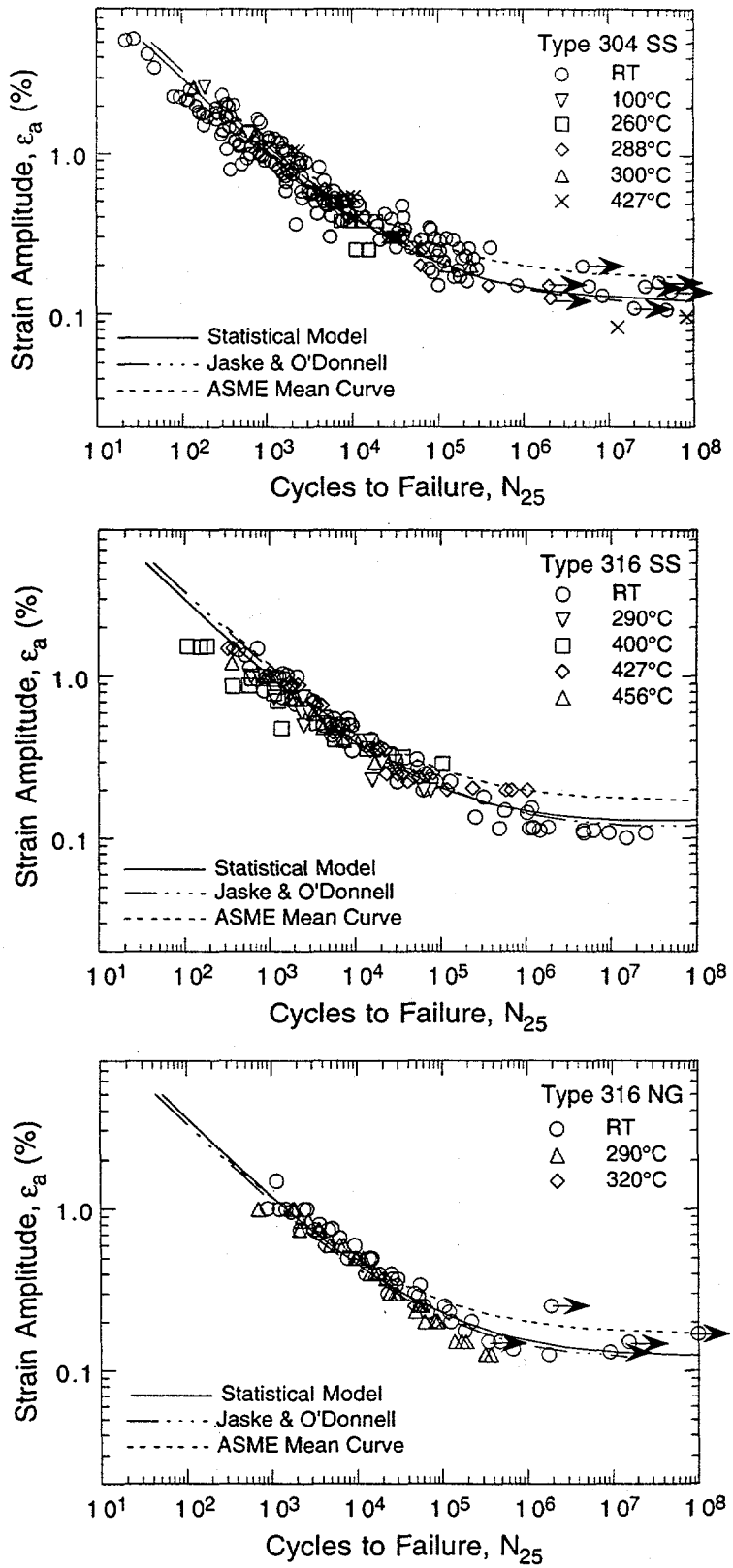

Figure 1. Fatigue S–N behavior for Types 304, 316, and 316NG austenitic stainless steels in air at various temperatures. Arrows represent run offs.

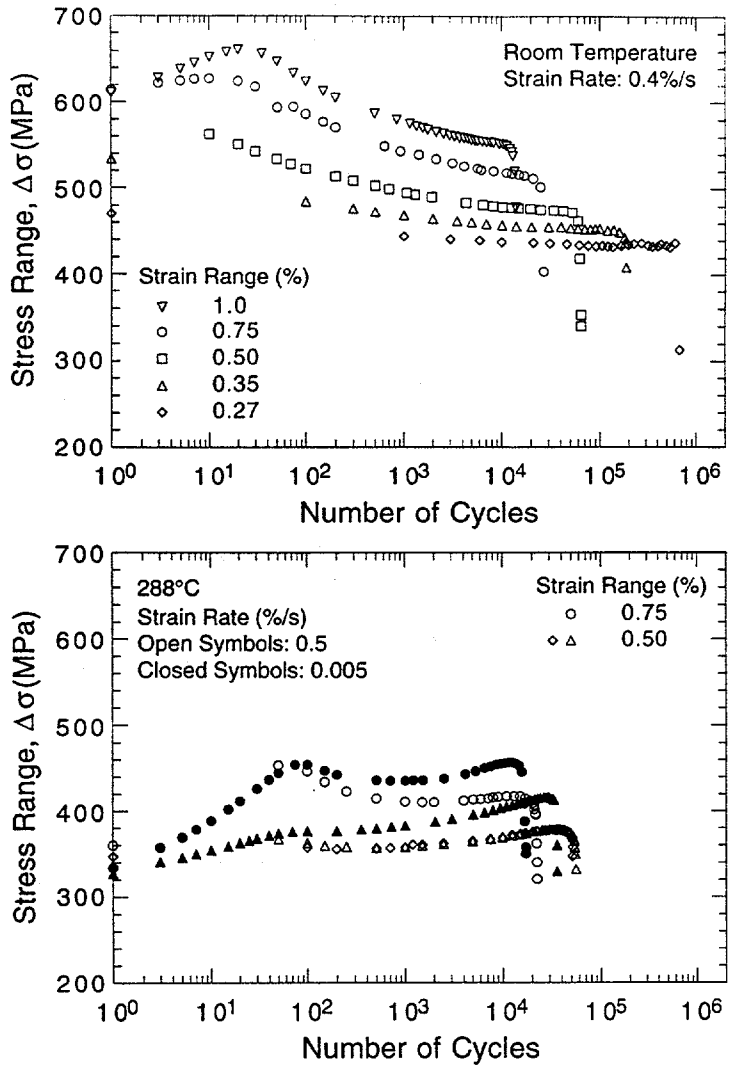

Figure 2. Effect of strain range on cyclic strain–hardening behavior of Type 316NG stainless steel in air at room temperature and 288°C

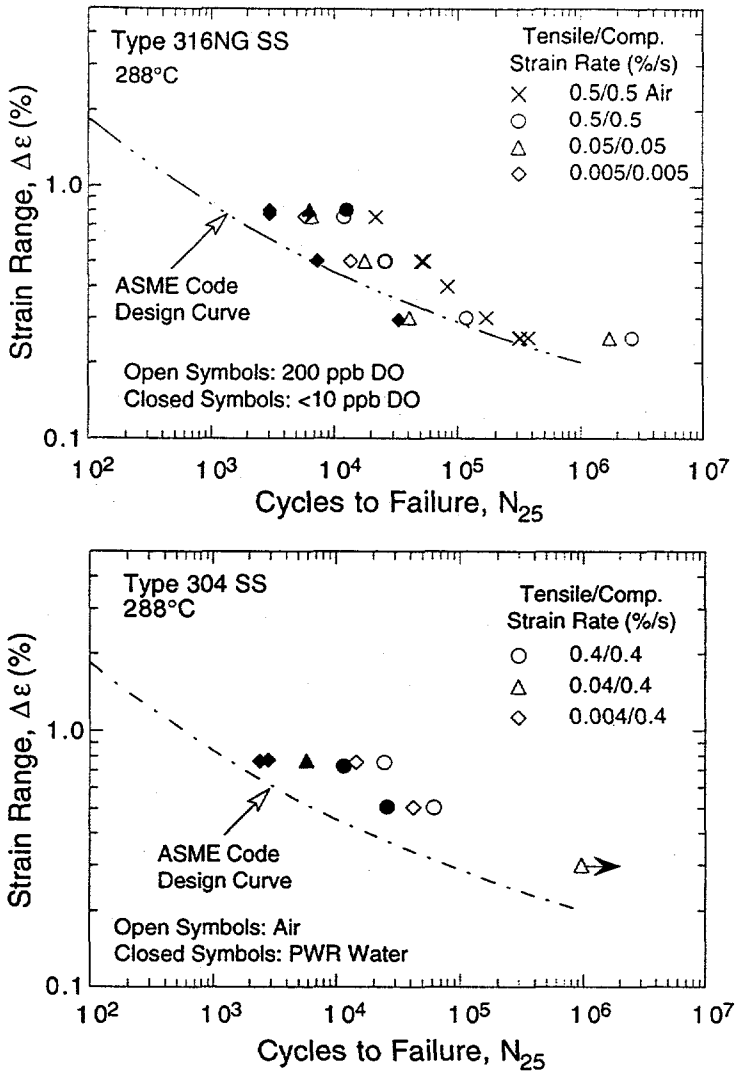

Figure 3. Total strain-range-vs.-fatigue-life data for Types 316 NG and 304 SS in air and water

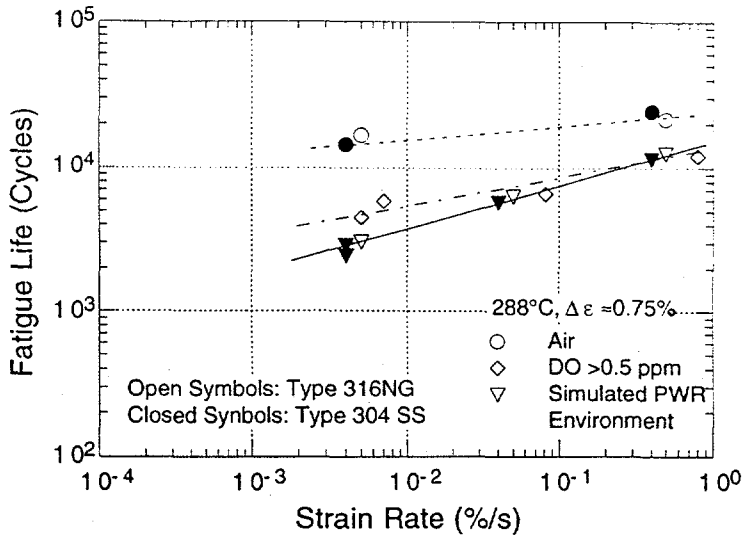

Figure 4. Effect of strain rate on fatigue lives of austenitic stainless steels in air, high-DO-water, and simulated PWR environments

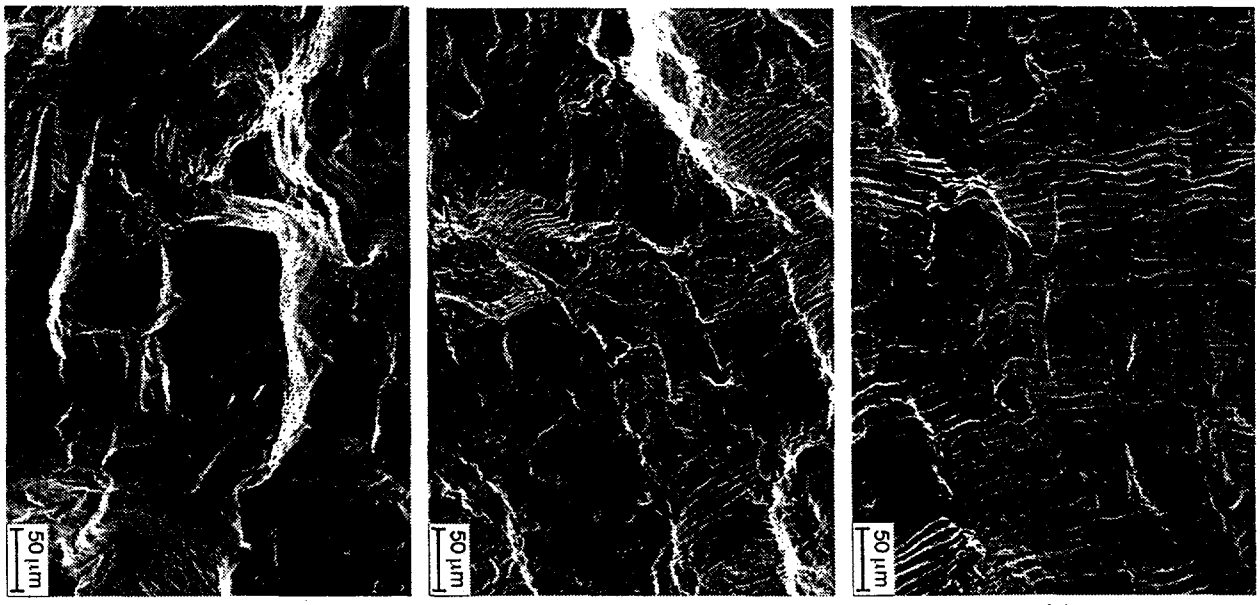

Figure 5. Photomicrographs of fracture surface of Type 316NG SS specimens tested at 288°C in (a) air, (b) high-DO water, and (c) simulated PWR water

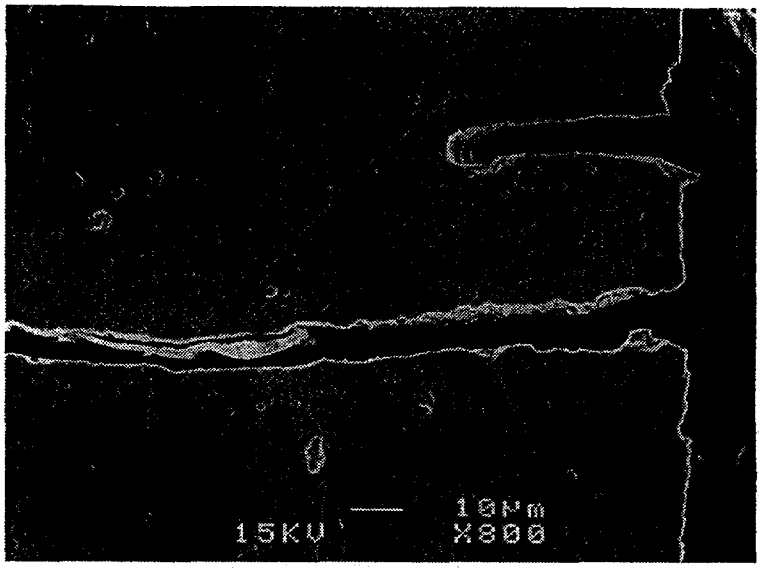

<0.01 ppm Dissolved Oxygen

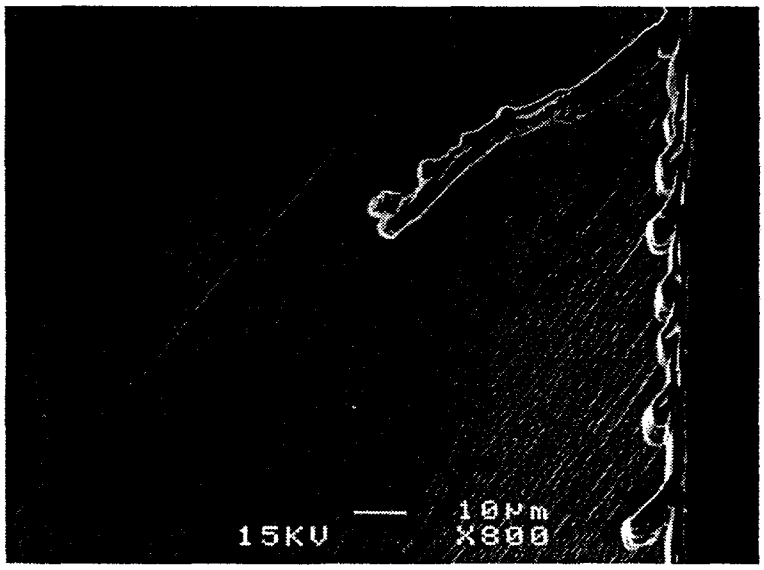

≈0.7 ppm Dissolved Oxygen

Figure 6. Photomicrographs of surface cracks along longitudinal sections of Type 316 NG stainless steel tested at 288°C in low- and high-DO water